INTERNATIONAL JOURNAL OF AUTOMOTIVE SCIENCE AND TECHNOLOGY

2022, VOL. 6, NO:4, 357-363 www.ijastech.org e-ISSN: 2587-0963

A Novel Engine Vibration Measurement System based on the MEMS Sensor

Ahmet Böğrek[1*], Harun Sümbül[2]

0000-0001-9767-9897, 0000-0001-5135-3410

[1] *Department of Automotive Technology, Yesilyurt Iron and Steel Vocational School, Ondokuz Mayis University, Samsun, 55300, Turkey*
[2] *Department of Biomedical Device Technology, Yesilyurt Iron and Steel Vocational School, Ondokuz Mayis University, Samsun, 55300, Turkey*

Abstract

Internal combustion engines cause the engine to vibrate with a certain acceleration due to the oscillation of many components and combustion events during operation. The resulting vibrations can give information about the regular operation of the engine or a possible mechanical failure. For this reason, it is very important to measure and interpret these vibrations in a healthy way.

In this study, a microcontroller-based measurement system was designed and implemented to examine the vibrations of a 4-stroke, 3-cylinder and water-cooled diesel engine at different speeds, under loaded and unloaded conditions. Vibration results for three different measurement points at different engine speeds (900,1200,1600,2000,2400,2800 and 3200rpm) were recorded in the data recording system for 60s. The recorded data were filtered by the EMA method and the results were analyzed by the FFT method.

According to the results obtained, it has been determined that there is a close linear relationship between engine speed and vibrations. Results of measurement point 1 (Cylinder head) Higher vibration harmonics were measured compared to measurement points 2 (engine block) and 3 (Flywheel housing). The highest vibrations occurred at 3200rpm under loaded and unloaded operating conditions. As a result; It has been seen that the measurement system developed using MEMs-based accelerometers can be successfully applied to measure engine vibrations.

Keywords: Engine Speed, FFT, MEMs, Vibration

Research Article

https://doi.org/10.30939/ijastech..1168298

Received 29.08.2022
Revised 27.09.2022
Accepted 21.10.2022

* Corresponding author

Ahmet Böğrek

ahmet.bogrek@omu.edu.tr

Address Department of Automotive Technology, Yesilyurt Iron and Steel Vocational School, Ondokuz Mayis University, Samsun, Türkiye

Tel:+903623121919

1. Introduction

While designing the internal combustion engine, it is necessary to take into account the basic consumer demands, such as torque, power and fuel consumption, as well as the parameters that increase the quality of vehicle use. Today, many engine designs are out of preference because they create more noise and vibration than their competitors during normal operation. The general cause of vibrations during the operation of an internal combustion engine is the change in in-cylinder pressure, the noise created by the lubrication gaps between the components, the piston moving up and down, the crank-connecting rod mechanism gaps to which it is connected, and the axial travel gaps in the parts [1, 2]. These vibrations of the engine can be described as typical nonstationary motion [3]. These vibrations, which occur during the operation of the engine, cause a decrease in driving comfort as well as fatigue of the coupling elements as a result of vibration. Acceleration sensors can detect motion, vibration, impact and shock. detects and measures acceleration caused by causes [4]. Today, acceleration sensors are used for many purposes, such as improving safety and driving characteristics [5]. In the literature, it is seen that a piezoelectric acceleration sensor designed to measure vibrations in the engine and transmission and the signals of an accelerometer produced for commercial purposes are compared [4]. In another study, in which the effects of fuel and oil used in the engine on vibrations were examined, it was observed that the vibrations that occurred during the tests were analysed with two 3-axis accelerometers placed on the crankshaft main bearings [6]. In the literature, it has been determined that the vibration intensity of the engine increases with increasing engine speed and load [2, 6-9].

Thanks to the designed measurement system created in this study, vibration data from 3 different measurement points of a 4-stroke diesel engine under loaded and unloaded operating conditions were examined. The specifications of the test engine are given in Table 1, and the technical specifications of the loading system are given in Table 2. During the tests, the engine speed was varied between 900 rpm and 3200 rpm, and the loaded measurements were made under full load conditions. This is done to ascertain the vibration changes at the lowest engine speed (800 rpm) and highest engine speed (3200 rpm) at which the engine can run when fully loaded, as indicated by the engine catalog. The lowest engine speed was increased by 100 rpm, and tests were conducted at 900 rpm, but since the engine occasionally emits smoke at 800 rpm,

which is the minimum engine speed when the engine is loaded, this was done. By running testing at 400 rpm changes, it was also hoped to assess how vibration would vary with major engine speed changes. It is thought that the working performance of the developed card was sufficient to meet the requirements of engine tests.

Table 1. Technical specifications of the test engine

Specifications	Units	Properties
Model	-	Lombardini LDW1003
Engine Type	-	4 stroke, Direct Injection
Number of cylinders	-	3
Cylinder volume	cc	1028
Bore–stroke	mm-mm	75-77,6
Compression ratio	-	22,8:1
Max. Power	kW	19,5

Table 2 Engine Test System Features

Manufacturer	NetFren
Type	DC Electric Dynamometer
Max. Load Power	22kW

2. Materials and Methods

In this study, a microelectromechanical system (MEMS)-based measurement system that can measure low amplitude high harmonic vibration signals occurring during engine operation was designed and implemented. MEMS-based sensors are one of the most frequently used sensor groups, from military purposes to the health sector [10, 11]. The vibration detector (ADXL345) block diagram used in this study is shown in Fig. **1**.

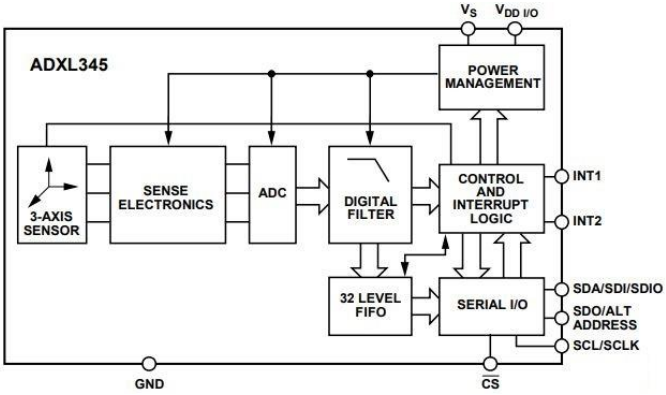

Fig. 1. Block diagram of the ADXL345 accelerometer [12]

The ADXL345 accelerometer is programmable within a measuring range of ±2 g, ±4 g, ±8 g, ±16 g. The measured data are saved as 2n, 2 bytes for each axis, for a total of 6 bytes. Depending on the selected measuring range, some bits in the most significant bit (MSB) of the axis data output are reserved as sign bits. The number of bits that need to be set for registers and read for each axis depends on the selected measuring range. To calculate the actual acceleration (a) from the measured axial acceleration information (g'), the measured values must be expanded by a scaling factor (S_a). This equation is given below [13].

$$\|a(x,y,z\| = g'.S_a \quad (1)$$

Two parameters are needed to determine the scale coefficient: the number of bits representing the original values and the range at which the measurement was made. The ADXL345 is manufactured with a 10-bit measuring range, but this range can be changed with appropriate software. The scaling coefficient is found as in Eq. (1). While "r" given in Eq. (2) is the total scale range, "n" is the number of resolution bits. However, the use of a scale factor of 3.90625 mg for all "g" values is recommended in the sensor catalogue. In this case, when the acceleration information in the X, Y and Z axes in the "g" unit is calculated for the sample data (11, 13, 256) read from the sensor, it was found to be 0.042 g for X, 0.05 g for Y and 1 g for Z.

$$S_a = \frac{r}{2^n} \quad (2)$$

This axis information applies to the accelerometer reference position where the XY axes are parallel to the ground and the Z axis is perpendicular to the ground. Therefore, when the accelerometer is moved in different directions, these values will change depending on the sensitivity of the accelerometer. (Fig. **2**-a).

Using the axis information (X, Y, Z), tilt and angle information (α, β, γ) can also be calculated based on a selected reference axis position (Fig. **2**-b). The reference position of the sensor is usually the position where the XY axes are parallel to the ground (0 g) and the Z axis is perpendicular to the ground (1 g). All calculated angles are 0° because at the reference position, 0 g is on the X and Y axes and 1g is on the Z axis. This situation is shown in Fig. **2**.

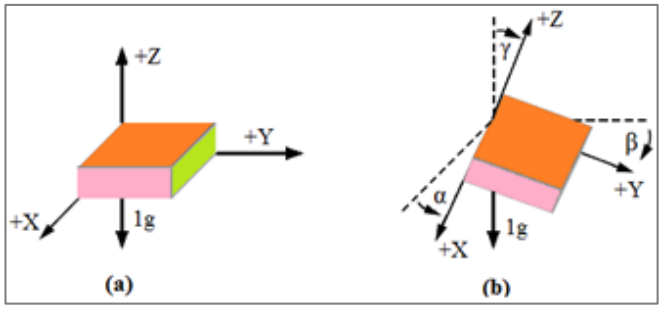

Fig. 2. Sensor reference position, a) sensor reference axis information, b) angle information between axes.

Sensor sensitivity is determined by a given supply voltage and is generally expressed in units of mV/g for accelerometers with analog output and in units of LSB/g or mg/LSB for accelerometers with digital output, such as the ADXL345. The unit'mg/LSB'

means milli 'g' per bit. For example, for a 10-bit accelerometer set in the 4 g measurement range, 10 bits gives a measurement value of 1023 (2^{10}=1023). Thus, each bit of the output value represents 4/1023 or 0.0039 g (3.9 mg). Thus, the output change for each bit value will be as seen in Table 3 below.

Table 3. Technical specifications of the test engine

No:	output values of the sensor (bit)	Acceleration Variables (g)
1	0000000000	**0**
2	0000000001	**0,0039**
3	0000000010	**0,0078**
4	0000000011	**0,0117**
5	0000000100	**0,0156**
6	0000000101	**0,0195**
7	0000000110	**0,0234**
8	0000000111	**0,0273**
…	…	**…**
1024	1111111111	**3,9897**

As seen, a one-bit change in LSB will always be reflected in the measurement result as 3.9 mg. Therefore, this term is expressed as 3.9 mg/LSB (approximately 4 mg/LSB).

The vector R is the combined force vector acting on the acceleration sensor. This force is given as the result of the gravitational force and the inertia force as a result of gravity or the movement of the sensor. If the 3 components of the R vector are expressed as R=[x',y',z'], according to the Pythagorean theorem;

$$R = \sqrt{x^2 + y^2 + z^2} \tag{3}$$

written with the relation. In this study, the resultant vector (R), whose equation is given for the data taken from different measurement points, is calculated and compared.

Due to its high sensitivity (4 mg/LSB), ADXL345 also allows the measurement of slope changes smaller than 0.25°. Band width: To detect acceleration changes in a slow-moving system, it should be 50 Hz and 100 Hz at high speed. The measuring range of the accelerometer used in the study was ± 157 m/s^2 (± 16 g), the sensitivity was 4 mg/LSB, the resolution was 10 bits, and the bandwidth was 100 Hz. The supply voltage is 3.3 V, and the current drawn is 150 µA.

The sampling frequency of the realized measurement system is 20 Hz. Each 10-bit data received consists of x, y and z data packets. Thus, the amount of data transferred is 20×3×10=600 bits/sec and is suitable for wireless transmission [14]. As seen in Fig. **3**, the system can be improved.

The measurement system circuit consists of a PIC 16F88 microcontroller, 2×8 character LCD display, accelerometer sensor (ADXL345), eeprom memory component (25LC512) and data transfer circuit board (FT232) [15]. The power required for the whole circuit is obtained from a circuit containing a 9 V battery and an LM7805 regulator. In the designed system, the ADXL345 is removed with an extension cable to increase the X-, Y- and Z-axis acceleration measurement accuracy.

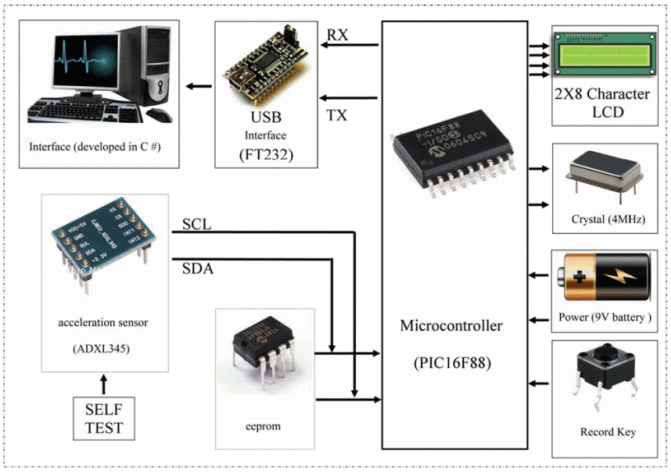

Fig. 3. Measuring system block diagram

The power required for the whole circuit is obtained from a circuit containing a 9 V battery and an LM7805 regulator. In the designed system, the ADXL345 is removed with an extension cable to increase the X-, Y- and Z-axis acceleration measurement accuracy.

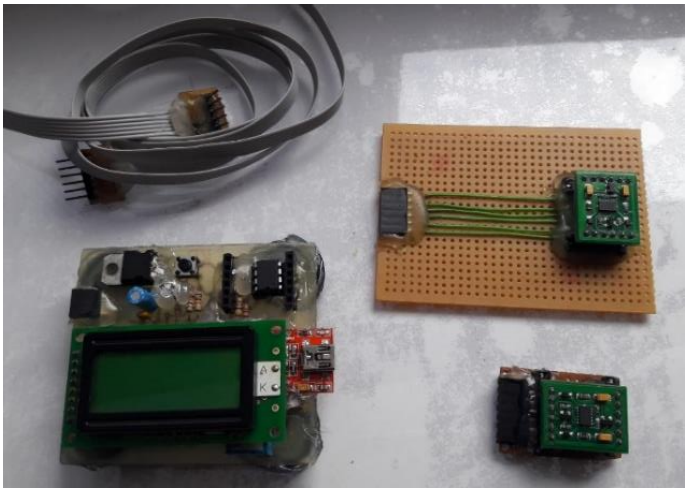

Fig. 4. Measurement System

The vibration measurement system, designed to measure vibrations occurring at different revolutions of the engine (900, 1200, 1600, 2000, 2400, 2800 and 3200), recorded signals from three different points for 60 seconds. In all tests, the engine was tested under full load conditions, and standard diesel was used as the test fuel. Fig. **5** shows the points where the accelerometer is connected to the engine.

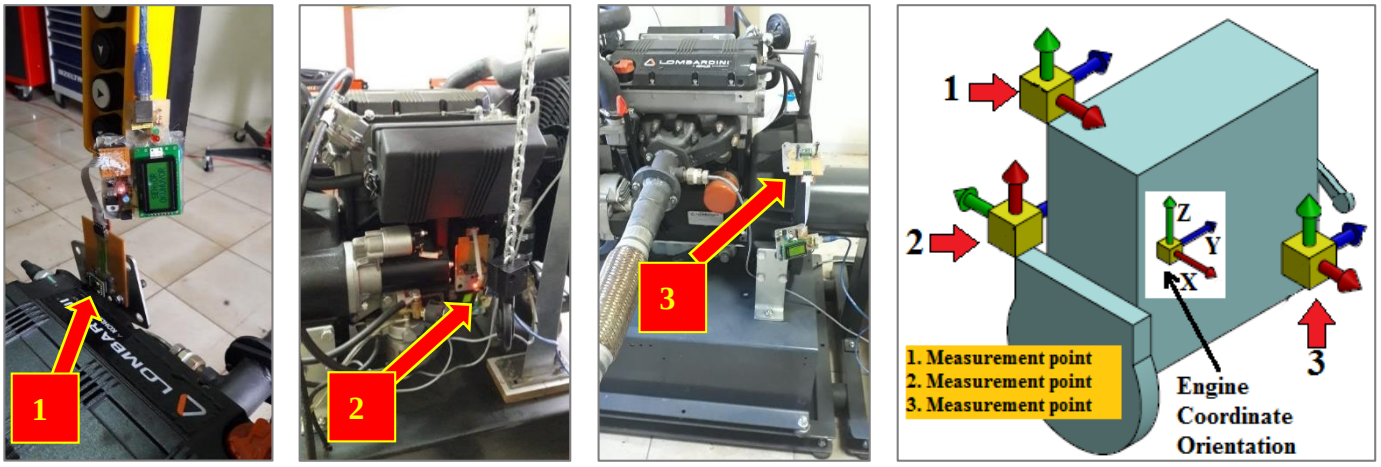

(a) Cylinder head (b) Engine block (c) Flywheel housing (d) Engine coordinate orientation

Fig. 5. Measuring points where the accelerometer is fixed

The first measuring point (1) is on the cylinder head. The second measuring point (2) is at a point close to the engine's crankshaft axis and is on the LBW axis of the 1st cylinder. The third measuring point (3) is in the flywheel housing, which is connected to the engine block. Since the acceleration sensor is connected in different positions at the measurement points, the sensor signals in all measurements are arranged according to the engine coordinate system.

The obtained data were transferred to the computer environment and analyzed by the Python program. The exponential moving average (EMA) is used to filter out noise in the measured vibration signals and identify trends. This method is a widely used method for filtering noise and identifying trends. In this method, the weight of each item gradually decreases over time, meaning that the exponential moving average gives more weight to the final data points. This is done under the idea that recent data are more relevant than old data. Compared to the simple moving average, the exponential moving average reacts more quickly to changes, as it is more sensitive to recent movements [16]. The equation used to calculate the exponential moving average at time T can be seen in Eq. (4):

$$EMA_t = \begin{cases} x_0 & t < 0 \\ \alpha x_t + (1-\alpha) EMA_{t-1} & t > 0 \end{cases} \quad (4)$$

where x_0 is the monitored value over time period t, EMAt, and t is the exponential moving average in the time period. α is the smoothing factor. The smoothing factor has a value between 0 and 1 and represents the weighting applied to the most recent period [17].

Finally, Fast Fourier transform (FFT) analysis, which has been very successful in recent years, has been performed on mechanical vibration signals. In this study, the FFT transform was preferred because it is the most widely used method in the literature in vibration analysis [18]. Fourier analysis is a tool used to reconstruct a periodic waveform using series harmonics, where the harmonic frequency is defined as a multiple of the fundamental and is used to convert a signal in the time domain to the frequency domain [19]. FFT is an algorithm that calculates the Discrete Fourier Transform (DFT) or inverse discrete transform of a sequence. The analytical equation for the Fourier transform is given below.

$$S_{x(f)} = \int_{-\infty}^{+\infty} x(t) e^{-j\pi f t} dt \quad (5)$$

Here, $Sx_{(f)}$ is the output of the Fourier transform in the frequency domain, $x_{(t)}$ is the time domain function and $2\pi f$ is the frequency in radians per second.

3. Results and Discussions

As a result of the tests performed, the resultant acceleration values with the engine speed under loaded conditions are presented in Fig. **6** (a, b and c). According to the filtered acceleration data, the measurement point where the highest harmonic signal is taken is point 1. The highest acceleration value was measured at 3200 rpm for all measurement points. For point 1, a nearly linear variation is observed between the engine speed and acceleration results. For point 2, although the acceleration results show a variable course at low engine speeds, linear vibration data are obtained at high speeds. In the results obtained from the 3-point data, irregular acceleration changes were observed. However, after the 20th second, the acceleration values became more linear. According to the loaded vibration results, the increase in engine speed caused the measured g-force to increase as well.

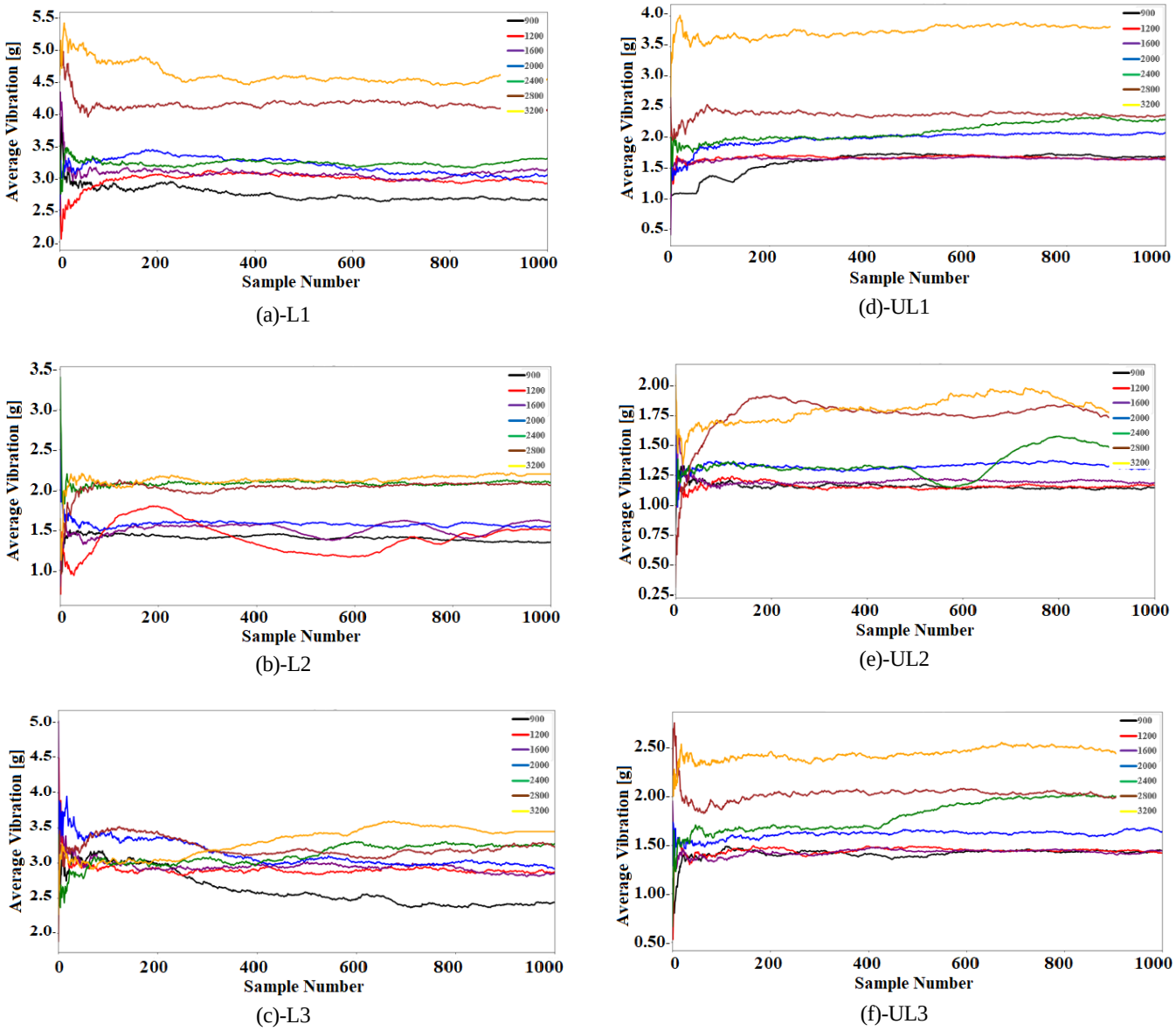

Fig. 6. Filtered acceleration results in loaded and unloaded conditions

The engine speed and vibration changes under no-load conditions are given in Fig. **6** (d, e and f). According to these results, the point where the highest vibrations are measured is point 1. In general, the vibration values show harmonious changes depending on the engine speed. However, acceleration values at low speeds (900-1200 and 1600) at points 2 and 3 under no-load conditions were quite close to each other. Acceleration results for 3200 and 2800, 2400 and 2000 rpm at point 2 showed close changes.

In Fig. **7**, changes in engine torque, engine speed and average acceleration are given. Vibration averages increased as the engine speed increased for both loaded and unloaded conditions. Under load conditions, the engine vibrates at a higher rate. The acceleration measured at point 1 is higher than the values taken from points 2 and 3. This is because the sensor connection point is at the longest distance relative to the distance the engine is fixed to the test bench. The lowest acceleration changes were detected at 2 points. In addition, the change in engine speed affected the vibrations more than the torque changes. Vibration values under load conditions were higher than vibration values under no load conditions. However, for point number 2, this change can be ignored. The number 2 point is because the engine is closer to the connection point to the test bench compared to other points.

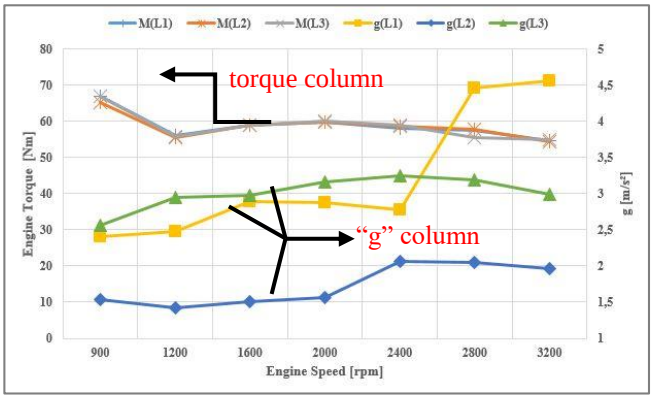

(a)-Loaded

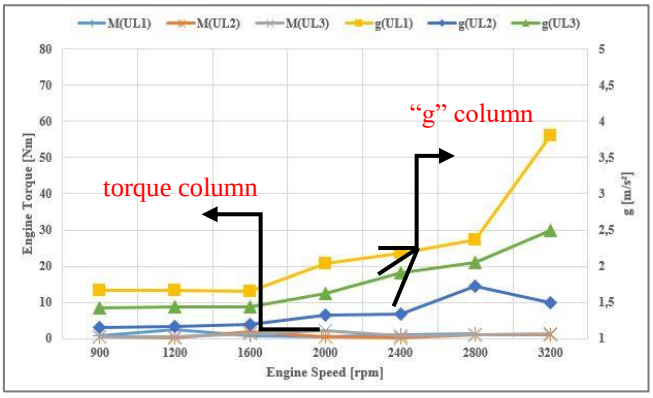

(b)-Unloaded

Fig. 7. Engine speed vibration relationship

Looking at the average vibration data, it is clearly seen that the average vibration value order of each point is 1>3>2. FFT analysis of the vibration data of point 1 under the loaded conditions where the highest vibration acceleration occurs is presented in Figure 8.

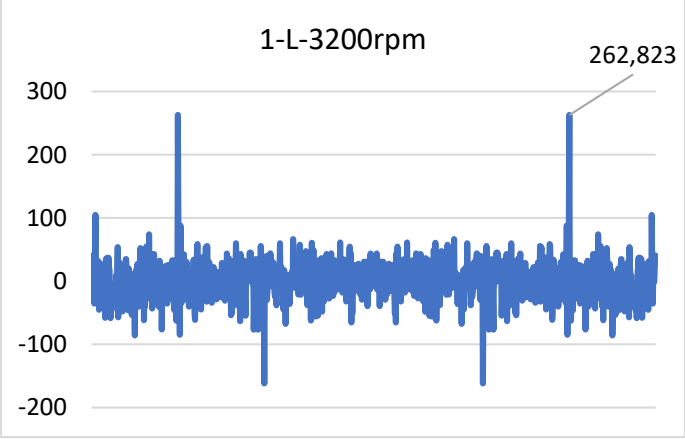

Fig. 8. Signal FFT at point 1 with engine loaded

The FFT value of the 3200 rpm rpm signal measured at point 1 under loaded conditions in Figure 8 shows a large peak at 945 Hz, resulting in an unpleasant sound. It is thought that this noise originates from the gap between the engine shaft and the dynamometer coupling connection point when loaded at high speeds. Low amplitude harmonics caused by high speed operation are seen on the graph.

In addition, the engine may resonate at high speed, and the engine and bearing may be damaged and fail. As a result, it was concluded that the signal cannot be analyzed without frequency spectrum analysis as a result of the difficulty of interpreting raw sensor data in vibration analysis. In future studies, we plan to develop a modern fault detection and diagnosis system based on vibration data by using machine learning methods.

4. Conclusions

In this article, a microcontroller-based measurement system has been designed and implemented to examine the vibrations of a 4-stroke, 3-cylinder and water-cooled diesel engine at different speeds under loaded and unloaded conditions. Vibration results were recorded in the data recording system for 60 s for three different measurement points at different engine speeds (900, 1200, 1600, 2000, 2400, 2800 and 3200 rpm). The recorded data were filtered by the EMA method, and the results were analyzed by the FFT method.

According to the results obtained, it has been determined that there is a close linear relationship between engine speed and vibrations. With the results of measurement point number 1 (Cylinder head), higher vibration harmonics were measured compared to measurement points number 2 (engine block) and number 3 (Flywheel housing). The highest vibrations occurred at 3200 rpm under loaded and unloaded operating conditions. As a result, it has been seen that the measurement system developed using MEM-based accelerometers can be successfully applied to measure engine vibrations. In future studies, it is planned to analyse engine vibration data with different artificial intelligence methods and to develop a measurement system for the detection of mechanical failures of engine components.

Acknowledgement

This study is supported by the Coordinatorship of Ondokuz Mayis University's Scientific Research Projects (Project No: PYO.YMY.1901.17.001), SAMSUN, TURKEY

Nomenclature

DFT	:	Discrete Fourier Transform
EMA	:	Exponential Moving Average
FFT	:	Fast Fourier Transform
LSB	:	Least Significant Bit
MEMs	:	Microelectro mechanical system
RPM	:	Revolutions per minute

Conflict of Interest Statement

The authors declare that there is no conflict of interest in the study.

CRediT Author Statement

Ahmet Böğrek: Writing-original draft, Conceptualization, Supervision

Harun Sümbül: Data curation, Writing-original draft, Validation, Formal analysis

References

[1] Ahirrao NS, Bhosle SP, Nehete DV. Dynamics and vibration measurements in engines. Procedia Manufacturing. 2018;20:434-9.

[2] Bonato M, Goge P, editors. Assessing the vibration fatigue life of engine mounted components. 2018 Annual Reliability and Maintainability Symposium (RAMS); 2018 22-25 Jan. 2018.

[3] Chen A, Dai X, editors. Internal combustion engine vibration analysis with short-term Fourier-transform2010 2010: IEEE.

[4] Gül M, Karaer M, Doğan A. Design of piezoelectric acceleration sensor for automobile applications. International Journal of Automotive Science And Technology. 2021.

[5] Bogrek A, Sumbul H. Development of driver analysis system to improve driving comfort and to reduce mechanical abrasion in vehicles. Teknik Bilimler Dergisi. 2019.

[6] Santana CM, Mautone J, Gutierrez J, Junior HA. Effect of fuel and lubricant on engine vibration. SAE Technical Paper. 2020;2020-01-1015.

[7] Tuma J, editor Phase demodulation of impulse signals in machine shaft angular vibration measurements. Proceedings of the InternationalConference on Noise and Vibration; 2003.

[8] Yaşar A, Keskin A, Yıldızhan Ş, Uludamar E. Emission and vibration analysis of diesel engine fuelled diesel fuel containing metallic based nanoparticles. Fuel. 2019;239:1224-30.

[9] Yıldırım H, Özsezen A, Çınar A. Vibration and noise depending upon engine speed in a diesel engine fueled with biodiesel. The 6th European Conference On Renewable Energy Systems; 25-27 June 2018; Istanbul/Turkey: ECRES; 2018.

[10] Khan AM, Young-Koo L, Lee SY, Tae-Seong K. A triaxial accelerometer-based physical-activity recognition via augmented-signal features and a hierarchical recognizer. IEEE Transactions on Information Technology in Biomedicine. 2010;14(5):1166-72.

[11] Sumbul H, Yuzer AH, editors. Development of diagnostic device for COPD: a mems based approach2017.

[12] Anonymous. Analog devices digital accelerometer ADXL345 2017 [Available from: http://www.sparkfun.com/datasheets/Sensors/Accelerometer/ADXL345.pdf

[13] Akbar MB. Design and prototype development of motion and shock sensing RF tags: Georgia Institute of Technology; 2012.

[14] Sumbul H, Yuzer AH, editors. Measuring of diaphragm movements by using iMEMS acceleration sensor. 2015 9th International Conference on Electrical and Electronics Engineering (ELECO); 2015 26-28 Nov. 2015.

[15] Sumbul H, Ozyurt O. Effect of high-heeled shoes on gait: a micro-electro-mechanical-systems based approach. World Academy of Science, Engineering and Technology, International Journal of Electrical, Computer, Energetic, Electronic and Communication Engineering. 2017;11:412-7.

[16] A.I. M. Python ile hareketli ortalamalar 2020 [Available from: https://towardsdatascience.com/moving-averages-in-python-16170e20f6c.

[17] Anitha S, Jayanthi P, Thangarajan R. Detection of replica node attack based on exponential moving average model in wireless sensor networks. Wireless Personal Communications. 2020;115(2):1651-66.

[18] Çeven S, Bayir R. Bir asenkron motorun mekanik titreşim sinyallerinin ölçülerek arıza analizinin yapılması. European Journal of Science and Technology. 2020:312-22.

[19] Lin HC, Ye YC, Huang BJ, Su JL. Bearing vibration detection and analysis using enhanced fast Fourier transform algorithm. Advances in mechanical engineering. 2016;8(10).